INTERNATIONAL JOURNAL ON SMART SENSING AND INTELLIGENT SYSTEMS

Research Article | DOI: 10.2478/ijssis-2026-0007 Issue 1 | Vol. 19 (2026)

Deep learning in public health: evaluating anemia detection methods

Neelu Jyothi Ahuja[1], Jyoti Upadhyay[2], Tanupriya Choudhury[1], Ashish Jain[1] , Bhupesh Kumar Dewangan[4,*] and Ketan Kotecha[3]

[1]School of Computer Sciences, University of Petroleum and Energy Studies (UPES), Dehradun 248007, India

[2]School of Health Sciences, University of Petroleum and Energy Studies (UPES), Dehradun 248007, India

[3]Symbiosis Centre for Applied Artificial Intelligence (SCAAI), Symbiosis International (Deemed University) (SIU), Symbiosis Institute of Technology, Lavale Campus, Pune 412115, India

[4]Symbiosis Institute of Technology, Nagpur Campus, Symbiosis International (Deemed University), Pune, India

*E-mail: bhupesh.dewangan@gmail.com

Received for publication August 23, 2025

Abstract

Anemia is considered as prevalent public health concern that mostly impacts children, expectant or recently gave birth mothers, adolescent females, and women going through menstruation. This work focuses on detecting anemia and classifying anemia and its type by blood cell image using machine learning models—the VGG16, InceptionV3, and DenseNet121 for early identification of anemia. The F1-score, recall, accuracy, and precision of the models were assessed after they were trained on a dataset of closer to 1000 images of blood cells. The accuracy obtained was 93.43% for the VGG16 model, 90.48% for DenseNet121, and 78.80% for the InceptionV3 model. The different evaluation metrics reveal the extent of success of each model at blood cell classification for early identification and detection of anemia and its type. The present work aims to experimentally establish machine-learning models as valuable instruments for the early identification and detection of anemia.

Keywords

anemia, machine learning, blood cell classification, early detection, health outcomes, VGG16, InceptionV3, DenseNet121

I. Introduction

Adolescent girls and women who are menstruating, pregnant, or have recently given birth to a child, and small children are the main groups affected by anaemia, which is a significant public health concern, as per the World Health Organization (WHO). It is a disorder that primarily affects mothers and children with a deficient amount of hemoglobin (Hb) or red blood cells (RBC). Too little Hb in the body prevents oxygen from reaching the organs and tissues, resulting in anemia [1]. According to WHO data from May 1, 2023, anaemia affects 37% pregnant women, 30% women aged 15–49 years, and 40% children aged between 6 months and 59 months [2], Additionally, an Hb level below 11.0 g/dL for pregnant women and below 12.0 g/dL for non-pregnant women is typically regarded as indicative of anemia [3]. Symptoms of anemia include fatigue, weakness, dizziness, sleepiness, etc., adversely reducing productivity in adults as well as having a negative impact on psychological and physical development in children [1].

The reasons for anemia may include infections (intestinal parasites, malaria, and hemoglobinopathies) and/or nutritional variables (iron deficiency, vitamins, and minerals may also result in anemic infection) [2]. Clinically, mean corpuscular volume (MCV) of blood is employed as a primary test to diagnose anemia by calculating the average size of RBCs. Usually, abnormal MCV counts suggest anemia, which is

categorized as macrocytic (MCV > normal), normocytic (MCV within normal), or microcytic (MCV < normal) [4]. Anemia can be temporary or chronic, ranging in severity from moderate to severe [5]. Anemia is associated with various conditions, including cardiovascular diseases (CVDs), diabetes, cancer, HIV/AIDS, and inflammatory bowel disease, Nephrotic syndrome, hemoglobinopathy, Schistosomiasis, and Ague. Furthermore, decreased skeletal muscle mass and bone density, decreased mobility and functional capacity, increasing risk of repeated falls, higher frailty, greater risk of associated comorbidities diseases, cognitive decline, and increased lethality are just a few of the negative health effects that anaemia in the elderly population can have [6].

Anemia etiology is complex, with causes including hemoglobinopathies, infections, and inflammation associated with chronic diseases, as well as particular Micronutrient deficiencies (iron, zinc, pyridoxine, vitamin B-12, vitamin A, riboflavin, and copper). In response to the COVID-19 pandemic, India has strengthened its vaccination equity efforts and responded to growing socioeconomic problems. However, the NFHS-5 results show that the trajectory of anemia among youngsters has reversed, indicating a growing challenge for the country's health and well-being [7]. Depending on the patient's features, anemia can occur with a frequency of 9%–69.6% in patients with a risk of heart failure. A timely diagnosis and course of treatment for anemia would help people understand their condition and find appropriate medical care, which would improve productivity and consequently the economy. A higher rate of anemia in the population has an impact on the physical and mental well-being of those who are affected [8]. Previous research surveys carried out in India found that among women of reproductive age (WRA), low socioeconomic level, lack of educational opportunity, increasing childbearing, life in rural regions, women belonging to lower social groupings, and insufficient nutritional consumption were related to anemia. Moreover, anemia was linked to low blood ferritin levels, which indicate iron deficiency, according to a study conducted in urban India. Notably, the majority of these studies concentrate on national population patterns [3].

Over the past 2 years, analyses have shown that COVID-19 prognosis is closely linked to comorbidities like hypertension, arrhythmias, diabetes, and CVDs. Recent studies examining the link between anemia and short-term lethality in COVID-19 patients have yielded inconsistent findings. Nevertheless, emerging evidence suggests that pre-existing anemia may elevate the risk of severe outcomes in COVID-19 cases. Given that anemia is a significant global health issue, it heightens the likelihood of hospitalization and mortality, particularly in COVID-19 patients who have additional comorbidities. This analysis aims to evaluate how common anemia is among COVID-19 patients and its impact on hospital lethality through a comprehensive review and/or meta-analysis [9].

Transmissions of SARS-CoV-2, causing COVID-19, have affected millions globally. While most cases are mild, up to 20% require hospitalization for pneumonia, intensive care unit (ICU) admission, and mechanical respiration. Severe COVID-19 involves a hyper-inflammatory state with elevated markers like CRP, IL-6, and ferritin, the latter indicating iron storage and inflammation. Increased ferritin levels in individuals diagnosed with COVID-19, correlate with disease severity, ARDS, and death. Inflammation alters iron homeostasis, reducing circulating iron and its availability for Hb production, leading to anemia of inflammation (AI). We investigated anemia prevalence and iron homeostasis in hospitalized COVID-19 patients and linked these factors to clinical outcomes [10].

This research employs a deep learning model to detect anemia by classifying blood cells into four types: neutrophils, monocytes, lymphocytes, and eosinophils. A dataset of 9,957 blood cell images was collected and preprocessed, with images resized to 320 × 240 pixels. We employed various deep learning architectures, including InceptionV3, EfficientNet, DenseNet, and VGG16, to train the model. The efficiency of our model was determined using recall, F1-score, precision, and accuracy metrics. This research aims to enhance early detection of anemia through accurate classification of blood cells, contributing to improved healthcare in rural populations.

II. Related Work

Machine learning techniques have been applied to autonomously diagnose anemia over the years. These techniques include individual machine learning classifiers, ensemble models, and deep convolutional models. In order to detect characteristics and patterns, analyze these patterns, and diagnose conditions based on the patterns, machine learning is utilized. Due to their excellent accuracy rates, these diagnoses or predictions have gradually replaced existing non-invasive procedures for the diagnosis of anemia. Table 1 illustrates a summary of significant research papers from the last decade, highlighting various deep learning models and their corresponding accuracies.

Table 1: Summary of significant paper for last decade

Year	Paper ref	Data set	Deep learning models	Accuracy (%)
2016	[12]	All four classifiers are trained with dataset of 500 instances.	ANN, DT, k-NN, and NB	96.63
2023	[13]	The datasets were collected from10 health facilities across the country	A machine learning approach was used to detect iron-deficiency anemia with the application of NB, CNN, SVM, k-NN, and DT algorithms	99.12
2023	[16]	The suggested technique makes use of time-domain analysis to determine the relationship between blood hemoglobin concentration and palm color variations brought on by applying and releasing pressure. Processed and analyzed is a smartphone camera sensor that captures the entire event of palm color changes produced by a bespoke gadget.	Dual-mode information fusion with pre-trained CNN models and transformer	96.29
2023	[11]	A specially constructed dataset of 2,592 pediatric palpebral images was used in the investigation	UCE, UNet+ +, FCN, PSPNet, and Link Net.	94.14
2023	[15]	After beginning with 527 datasets, the experiment added 2,635 more by utilizing translation, flipping, and rotation.	CNN, k-NN, Naive Bayes', SVM, and DT were used to build the suggested models for the identification of anemia.	99.92
2024	[14]	The proposed study used a larger size of dataset of 527 conjunctiva images and was then augmented to 2,635	Machine learning algorithms such as CNN, k-NN, NB, DT, and SVM were utilized for the study to detect anemia	98.45

ANN, artificial neural network; CNN, convolutional neural network; DT, decision tree; FCN, fully convolutional network; k-NN, k-nearest neighbors; NB, Naïve Bayes; PSPNet, pyramid scene parsing network; SVM, support vector machine; UCE, unified convolutional encoder.

Dhalla, Sabrina, et al. investigated unified convolutional encoder (UCE), Nested U-Net (UNet+ +), fully convolutional network (FCN), pyramid scene parsing network (PSPNet), and Link Net, five deep learning-based architectures. A specially constructed dataset of 2,592 pediatric palpebral images was used in the investigation. Comparing the Link Net architecture to those of its competitors, the experimental results demonstrate that it performs the best. The results indicate that it scored 90.14% intersection-over-union (IoU), 93.78% dice score performance parameter, and 94.17% accuracy [11].

The machine learning classifiers used to categorize the dataset were decision tree (DT), artificial neural network (ANN), Naïve Bayes (NB), and k-nearest neighbors (k-NN); Dalvi & Vernekar provided a comparison study of their performance. With an accuracy of 96.63%, ANN outperformed the other individual classifiers, while k-NN had the lowest accuracy. Additionally, the Stacking ensemble learner surpassed the ANN with 92.12% accuracy when applied to the DT and k-NN for the goal of diagnosing anemia [12].

This study employs various machine learning algorithms, such as support vector machine (SVM), convolutional neural networks (CNN), k-NN, DTs and naive Bayes, were utilized to recognize iron deficiency anemia. These methods examined the color of fingernails the texture of the palms and/or the appearance of the eye conjunctiva to establish an approach for detecting anemia in children. The process involved three stages: collecting dataset, analyzing the datasets, and developing effective models for identifying

anemia. The CNNs achieved a higher Precision of 99.12% compared to SVM with 95.6% [13].

The anemia in children is identified using conjunctiva images via machine learning techniques like CNNs, SVM, k-NN, DT, and NB. Initially, images are segmented into distinct CIE Lab (CIELAB) color space component and therefore ROI was obtained for every image. The datasets were then randomly partitioned into 70:10:20 and the model was trained, tested, and validated carefully. CNN exhibited highest accuracy rate at 98.45% [14].

The methodology of this study is broken down into three stages as follows: In the beginning, the dataset for palm was collected, followed by inclusion and processing of the acquired images. Additionally, these images were extracted and significantly enhanced. The region of interest was carefully segmented, and various CIELAB color space were collected. Finally, several algorithms mentioned above were utilized to build the models for the successful identification of anemia. After beginning with 527 datasets, the experiment added 2,635 more by utilizing translation, flipping, and rotation. The study's findings are consistent with the theory that the models performed as intended when anemia was diagnosed using the images of the palms of the subjects. The NB model demonstrated the best accuracy at 99.96%, while the SVM model exhibited the lowest accuracy of 96.34%. With a 99.92% accuracy rate, the CNN model was even more successful at diagnosing anemia [15].

The proposed method uses video data of palm pallor changes captured by a smartphone and a customized device to diagnose anemia. Keyframes are extracted at specific timestamps: initial color, maximum fading, and color return. These frames are processed using pre-trained models and a vision transformer (ViT) to capture essential features. Feature-level fusion combines these features, enhancing the model's representation. Multi-layer perceptron (MLP) heads handle classification and regression tasks. Majority voting is used for classification, while weighted averaging estimates Hb levels. This approach leverages deep models and ViT for improved classification accuracy and precise Hb estimation [16].

Numerous artificial intelligence exist, including Support Naive Bayes, Multilayer Perceptron Decision Tree, k-NN, SVM, Average Ensembles, random forest (RF), Hybrid Classifiers, and genetic algorithm (GA)-CNN. Several research works have investigated the significance of machine learning in classifying various forms of anemia, as exemplified by [17–19], which utilized data such as complete blood count (CBC) to develop models for anemia detection.

In Bangladesh, Anemia is considered a serious public health concern, particularly for youngsters. It is imperative to predict this condition to organize healthcare resources and create community health policies that work. The main objective of this research was to identify a machine learning technique for predicting anemia in children <5 years based on typical risk factors identified in the study dataset from the 2013 Bangladesh Demographic and Health Survey (BDHS). The study evaluated six machine learning methods using metrics such as confusion matrix analysis, as well as accuracy levels and sensitivity and specificity measures to assess their effectiveness. The study evaluated six methods: logistic regression (LR) classification and regression trees (CART) SVM RF linear discriminant analysis (LDA), and k-NN. The results indicated that the CART technique outperformed the rest with top scores of 62.35%, 71.54%, and 53.52% [18].

To improve the precision of the identification process necessary to merge learning and machine learning methods together effectively. We utilized CNNs stacked autoencoders (SAEs) and GAs. These techniques were used to forecast types of anemia, such as iron or dietary deficiencies related anemia and deficiencies in folate and B12 levels, while also differentiating individuals without the condition involved in the study. The model's performance was assessed using a confusion matrix. The GA-CNN method achieved an accuracy rate of 98% the F1 score of 98%, the precision level of 99% and the sensitivity score of 98% [20].

A machine learning method for identifying anemia using pictures of the conjunctiva in the eye was presented by Chen et al. [21] Using these photos for training and testing, the system reached a 95 percent confidence interval. Similarly, by examining the relationship between emotional tweets and anemia symptoms, Sarsam et al. [22] developed a novel technique for diagnosing anemia. Utilizing the k-means and latent Dirichlet allocation techniques, their study produced a 98.96% prediction accuracy.

In a study by Yeruva et al. [23]. used the DT, SVM, and k-NN algorithms for analyzing images of individuals with and without anemia to determine anemia. Hb levels were incorporated from blood samples as a dataset for their investigation, which involved examining photographs of the conjunctiva in the eye. To improve the quality, the images were preprocessed, noise filtering, and grayscale. The DT approach

outperformed the SVM and k-NN methods, with accuracy rates of 95%, 80%, and 83% respectively.

To detect the anaemia most of the researchers used non-invasive method such as using the patient's pictures of their conjunctive eyes, color of the fingernails, palpable palm, and tongue. In an elegant study, Tamir et al. [24] SVM was utilized to analyze conjunctive images to develop a non-invasive approach for anemia detection. Using 19 photos with known Hb levels, the study obtained 78.90% accuracy, correctly diagnosing 15 out of the 19 cases as anemia.

Wang et al. [25] presented a method in 2017 that enables simultaneous feature selection and parameter optimization by fusing the extreme learning machine of Kernel with the chaotic moth-flame optimization approach. This method was effectively used on datasets related to breast cancer and Parkinson's illness. Later, in 2020, Wang and Chen [26] combined the SVM approach with the whale optimization algorithm (WOA), where the SVM method's efficiency in parameter optimization and feature selection was improved by a multiswarm, chaotic algorithm. They reported positive results after using this technique on datasets for erythematous-squamous diseases, diabetes, and breast cancer.

Machine learning methods, including individual classifiers, ensemble models, and deep convolutional networks, have been increasingly utilized for diagnosing anemia due to their high accuracy rates. Various deep learning architectures, such as UCE, UNet+ +, FCN, PSPNet, and Link Net, have been tested, with Link Net showing the best performance using a pediatric palpebral image dataset, achieving 94.17% accuracy. Studies comparing machine learning classifiers like ANN, DT, k-NN, and NB found ANN to be the most effective. Ensemble learners further improved diagnostic accuracy. Non-invasive techniques using images of fingernails, palpable palms, and conjunctiva have been highly successful, with CNN models achieving up to 99.96% accuracy. A smartphone-based method using video data of palm pallor changes, combined with ViT and MLP, demonstrated improved diagnostic precision. Research in Bangladesh highlighted the severe public health issue of anemia among children, employing machine learning methods for effective prediction and resource planning. Hybrid approaches combining GAs, SAEs, and CNNs have shown outstanding performance in diagnosing various types of anemia. Additionally, studies have used conjunctiva images, Twitter posts, and enhanced image datasets for reliable anemia detection, with DT algorithms often outperforming others. Advanced optimization strategies like the chaotic moth-flame and WOA have further enhanced the accuracy of SVM methods in medical datasets.

III. Material and Methods

In the present work, a model is trained on 9,957 blood cell images categorized as (neutrophils, monocytes, lymphocytes, and eosinophils) to detect anemia. Once the image of blood cell is given to the trained model, the model classifies it on the basis of the image feature given during training set. The deep learning model extracts features from input images, enabling it to understand patterns and distinguish between categorized images. In this study, InceptionV3, EfficientNet, DenseNet, and VGG16 models have been used for training.

The figure of the present work comprises training the deep learning model to detect anemia by categorizing blood cells into neutrophils, monocytes, lymphocytes, and eosinophils based on features extracted from cell images (Figure 1). Pre-trained weights from the dataset were adjusted using deep learning architecture to adjust the model's characteristics for classifying anaemia. The model acquired the ability to differentiate between various types of anaemia by feature extraction from their images. The model's effectiveness was evaluated through evaluation measures including precision, accuracy, F1-score, and recall, ensuring its dependability and efficiency. The trained model was put to use in real-time after validation.

a. Dataset collection

In Uttarakhand, we identified three blocks in Dehradun District for our study: Vikasnagar, Doiwala, and Sahaspur (Figures 2-9). According to the 2011 Census, Vikasnagar has a population density of 13,927, with 7,128 males and 6,709 females. Doiwala has a population density of 8,709, with 4,659 males and 4,050 females. Sahaspur has a population density of 8,841, with 4,665 males and 4,176 females. Blood cell image data has been collected from these blocks through anonymous laboratories. A total of 9,975 blood cell images have been obtained, categorized as neutrophils, monocytes, lymphocytes, and eosinophils, using hematology microscopes. The focus of the data collection was primarily on women and children. This data will be instrumental in training our deep learning model

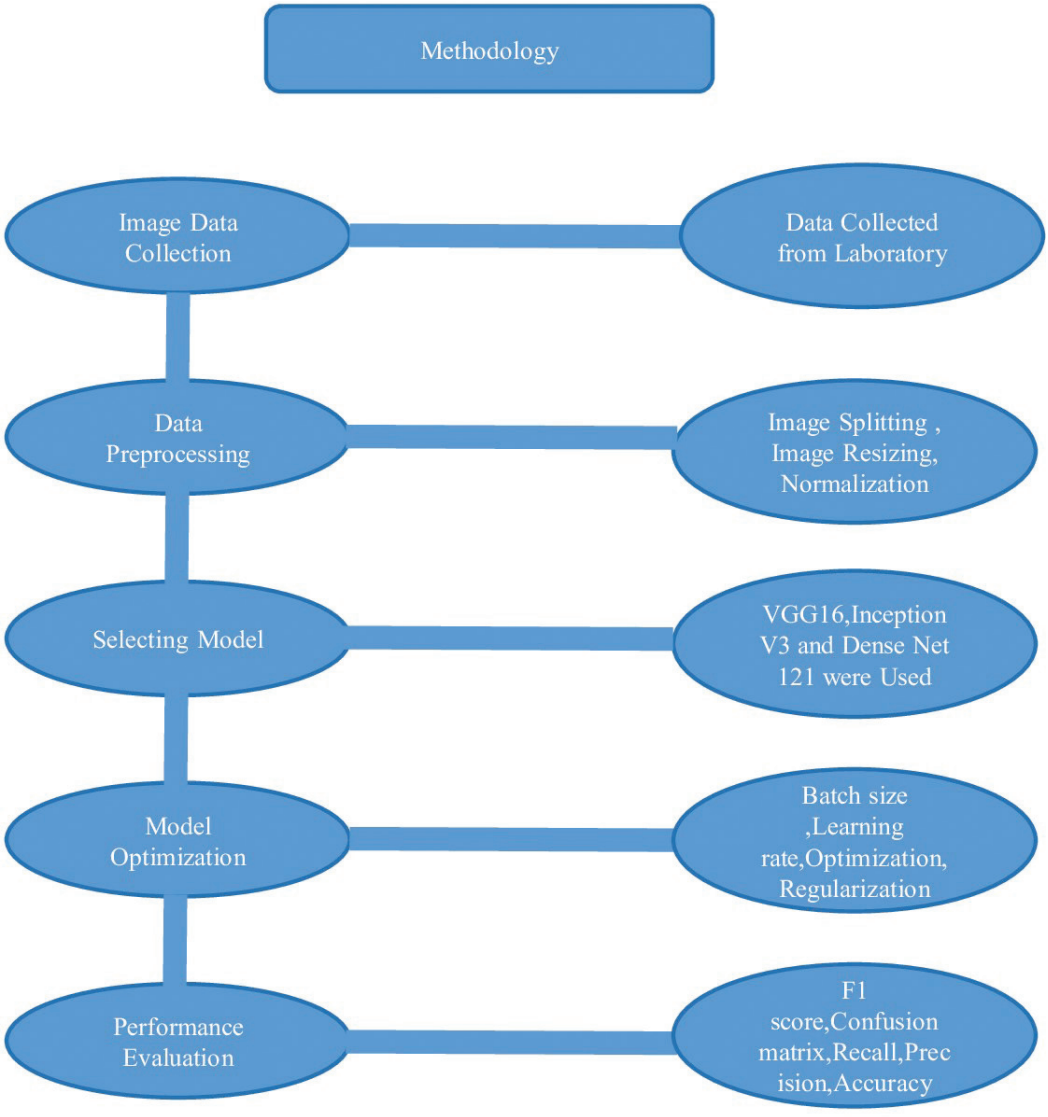

Figure 1: Methodology.

to detect anemia and provide insights into the health conditions of these specific demographics within the identified regions.

The dataset was labeled with the corresponding blood cell types. Three deep learning architectures—VGG16, InceptionV3, and DenseNet121—were identified due to their proven efficiency in image classification tasks. Evaluation Metrics such as accuracy, recall, precision, and F1-score were applied to evaluate the model's efficiency and present a complete evaluation of its blood cell type classification capabilities.

b. Data pre-processing

Several techniques were applied to achieve optimal effectiveness of the deep learning model when pre-processing anemia images, as illustrated in Figure 10. The images were resized to 320 × 240 pixels and converted into NumPy arrays for efficient processing. Image normalization was performed to standardize the pixel values, improving the model's convergence. Data augmentation methods like flipping, rotation, and zooming were utilized for diversifying the training set and preventing overfitting. The dataset was separated into training and validation sets in an 80:20 ratio. To balance

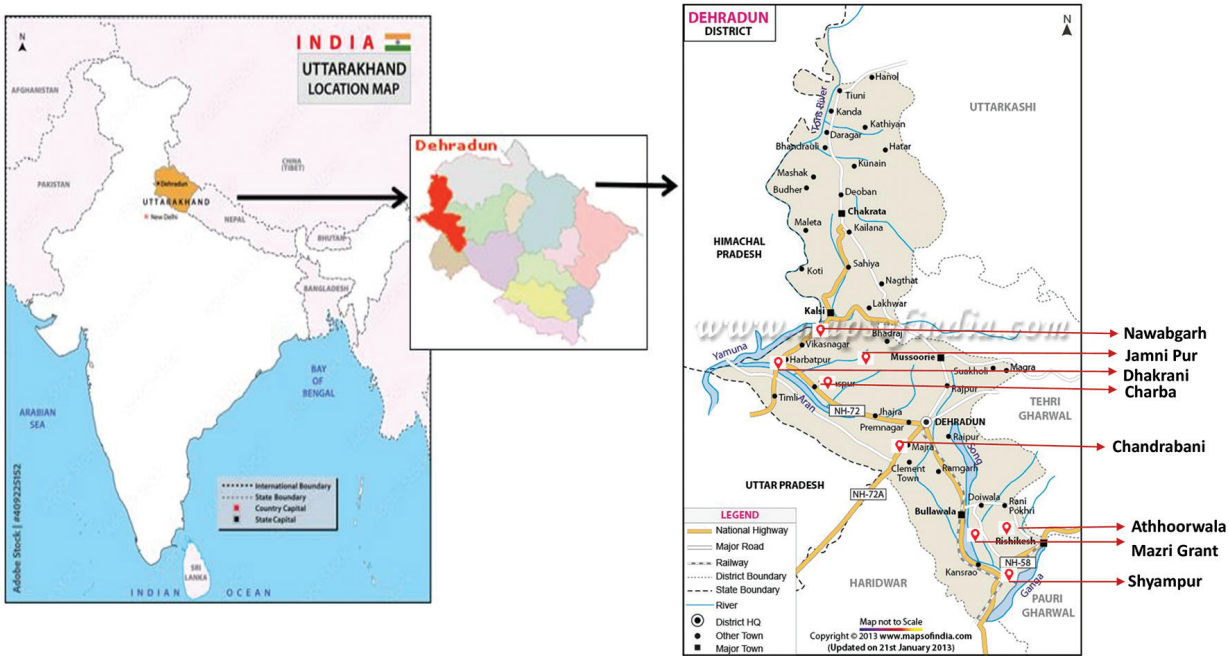

Figure 2: Site location in Dehradun district.

Figure 3: UPES to Dakrani.

computational efficiency with learning stability, a batch size of 32 was applied during training. To ensure smooth convergence, a learning rate of 0.001 was selected. These preprocessing steps were crucial for enhancing the model's capability to accurately classify blood cells and detect anaemia. Evaluation metrics were then performed to investigate the model's effectiveness and ensure its reliability in real-world practical applications.

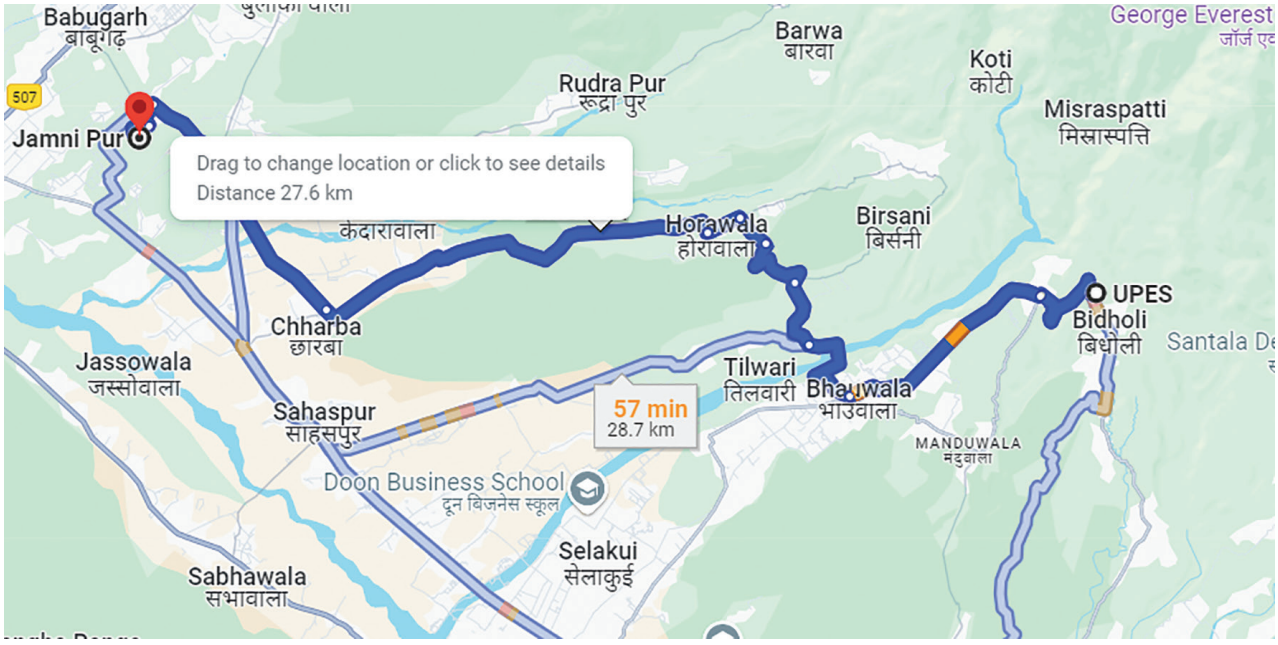

Figure 4: UPES to Jamnipur.

c. Data augmentation

c.i Diverse training data

Geometric transformations involve mathematical operations such as rotation, translation, and reflection. Given an original image ($I(x, y)$) and transformation parameters P, the augmented image I' is obtained as:

$$I'(x,y) = I(P(x,y)) \tag{1}$$

d. Convolutional layers with ReLU activation

Feature Extraction Given an input feature map X and a learnable kernel W, the convolution operation with ReLU activation is defined as

$$Conv\ (X,\ W) = \mathrm{ReLU}\left(\Sigma_i \Sigma_j X(i,j) \cdot W(i,j)\right) \tag{2}$$

This extracts hierarchical features from pre-processed lung images, capturing spatial hierarchies crucial for classification.

e. Deep learning model

A pre-trained deep learning model was precisely refined to categorize anemia into four categories: neutrophils, monocytes, lymphocytes, and eosinophils. The dataset included 9,975 images of blood cells collected from the laboratory. By leveraging the existing capabilities of the pre-trained model, the fine-tuning of the model allowed it to adapt and adjust to the specific features of the blood cell images, improving its accuracy and efficiency in classifying these categories.

e.i CNNs

CNN is a deep learning model. Which is employed in Image recognition. CNN is the most used model in deep neural networks. It used convolution layers, also called hidden layers. These hidden layers work as filters. And used for training and testing the data, then gives output. CNN works on many types of models, here only one model is discussed, which is Vgg16 [27]. The Figure 11 shows the CNN architecture.

e.ii VGG16 model

The methodology began with preprocessing images by resizing them to 320 × 240 pixels to ensure uniformity and reduce computational complexity. The dataset was then divided into validation, training, and test sets, facilitating model training, hyperparameter tuning, and performance evaluation. Categorical labels

Figure 5: UPES to Atthorwala.

were one-hot encoded, transforming them into vectors suitable for multi-class classification. The VGG16 architecture, known for its effectiveness in image classification, was chosen as the base model, leveraging pretrained weights on ImageNet. To retain the high-level feature extraction capabilities of VGG16, its layers were frozen, preventing their weights from being updated during training. Custom layers were added on top of the frozen VGG16 layers to tailor the model to the specific task of blood cell classification. The model was compiled using the accuracy metric, sparse categorical cross-entropy loss for multi-class classification, a learning rate of 0.0001 for stable updates, and the Adam optimizer for its efficiency in training deep neural networks. The training was conducted with a batch size of 32 over 90 epochs, and the model weights were saved to preserve the best-performing model. Evaluation metrics included a confusion matrix, which detailed true negative, true positive, false negative, and false positive predictions for each class, and various

Figure 6: UPES to Nawabgarh.

plots, such as accuracy and loss curves, to visualize the model's training progress and effectiveness. These steps collectively ensured a robust and effective model for classifying blood cells and their types. Figure 12 presents the detailed architecture of the VGG16 deep learning model used in this study.

e. iii InceptionV3 model

In this study, we employed the InceptionV3 model to classify images of the blood cells (neutrophils, monocytes, lymphocytes, and eosinophils). A dataset with 9,957 images of blood cells was used to train the model of 320 × 240 pixels and convert them into NumPy arrays. The dataset was split into 80% and 20% in training and testing sets, respectively, with class labels encoded using label encoding. The top layer of the InceptionV3 model—which had been pre-trained on ImageNet—was eliminated. For 90 epochs, the model was trained. After saving the weights, the model was assessed using the test set, and a high-accuracy result was produced. The efficiency of the model was evaluated using evaluation metrics, for instance confusion matrix. The Inception-V3 pre-trained model, introduced by [28], includes over 20 million parameters and was developed by leading hardware experts in the industry. Each of the symmetrical and asymmetrical building blocks that make up the model includes different average and max pooling layers, convolutional layers, dropout layers, fully connected layers, and concatenation layers. Furthermore, batch normalization is usually done to the activation layers' input. The model uses SoftMax for classification. Figure 13 presents a schematic diagram of the Inception-V3 model.

The Inception-V3 pre-trained model, introduced by [28], includes over 20 million parameters and was developed by leading hardware experts in the industry. Each of the symmetrical and asymmetrical building blocks that make up the model includes different average and max pooling layers, convolutional layers, dropout layers, fully connected layers, and concatenation layers. Furthermore, batch normalization is usually done to the activation layers' input. The model uses SoftMax for classification. Figure 11 presents a schematic diagram of the Inception-V3 model.

Figure 7: UPES to Mazri Grant.

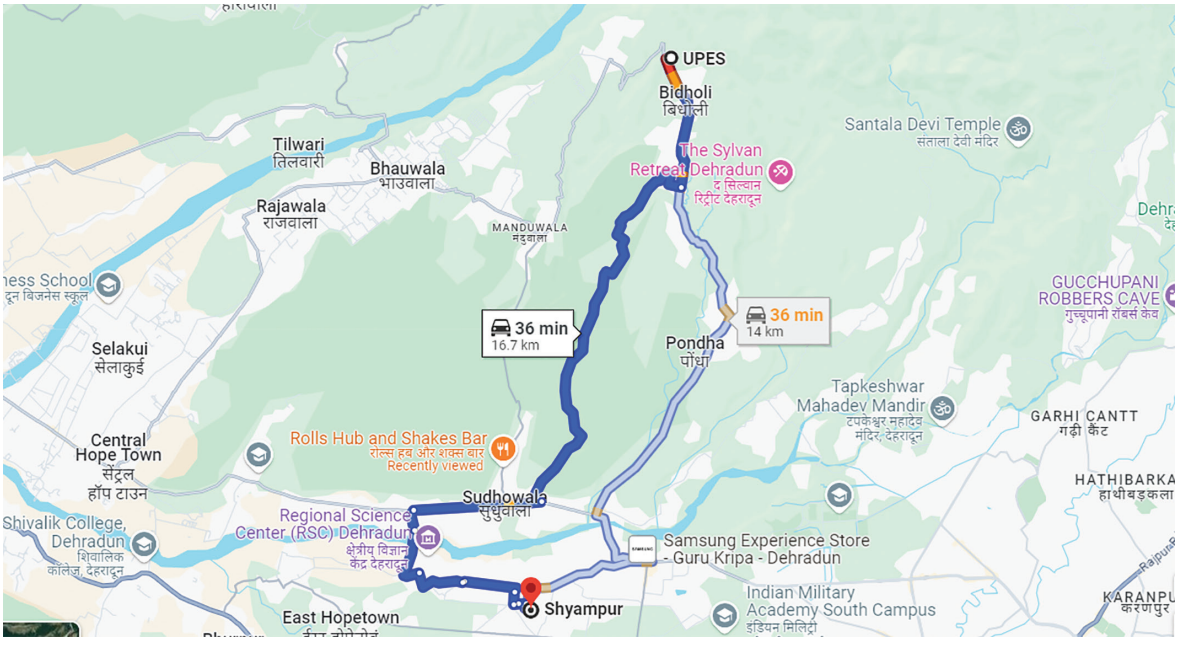

Figure 8: UPES to Shyampur.

Figure 9: UPES to Charba.

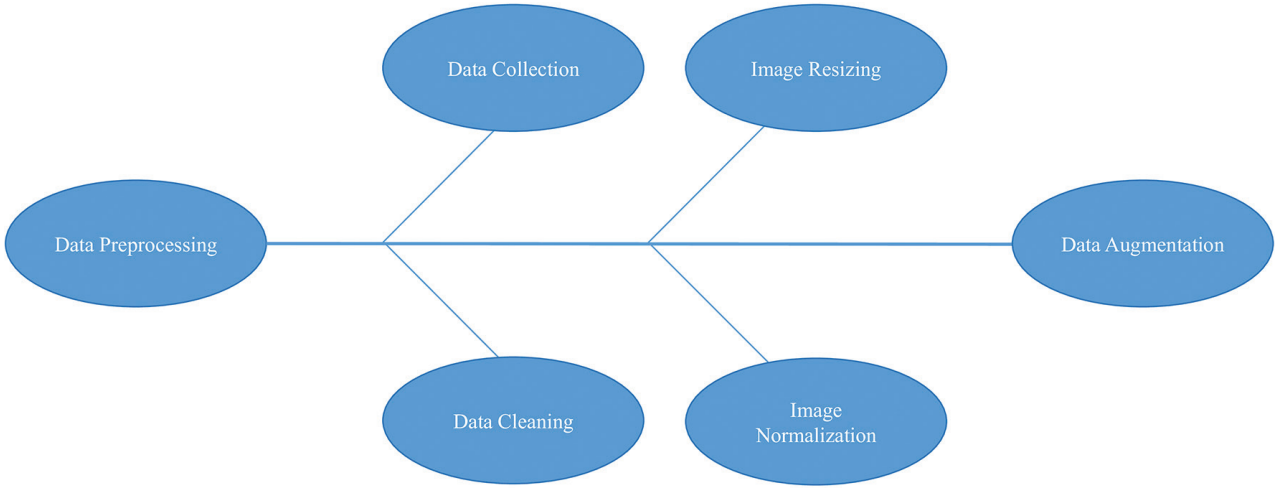

Figure 10: Data preprocessing.

f. DenseNET121

We employed the DenseNet121 architecture for image classification. The dataset consisted of images of the blood cells, with each image resized to (320, 240) pixels. We utilized transfer learning by loading the pre-trained DenseNet121 model without the top classification layer. The model achieved high accuracy on the test set after 90 epochs of training with a batch size of 32. We saved the model weights and evaluated its efficiency using various metrics, including classification accuracy, loss, and a confusion matrix was applied to measure the model's effectiveness. The Applied mechanism for predicting is shown in Figure 14.

g. Blood

As indicated in Table 2 [29], all of the body's blood cells are descended from bone marrow-derived pluripotent stem cells. RBC's main jobs include removing carbon dioxide from the body and carrying oxygen from the lungs to the tissues [30]. RBC typically have a lifespan of about 4 months, while platelets, which play a crucial role in hemostasis, circulate for approximately 10 days [31, 32]. White blood cells are composed of different types of phagocytes, including eosinophils, monocytes, neutrophils, basophils, and lymphocytes [33]. T cells are involved in regulating immune reactions, defending the body against viruses and foreign cells, while B cells produce

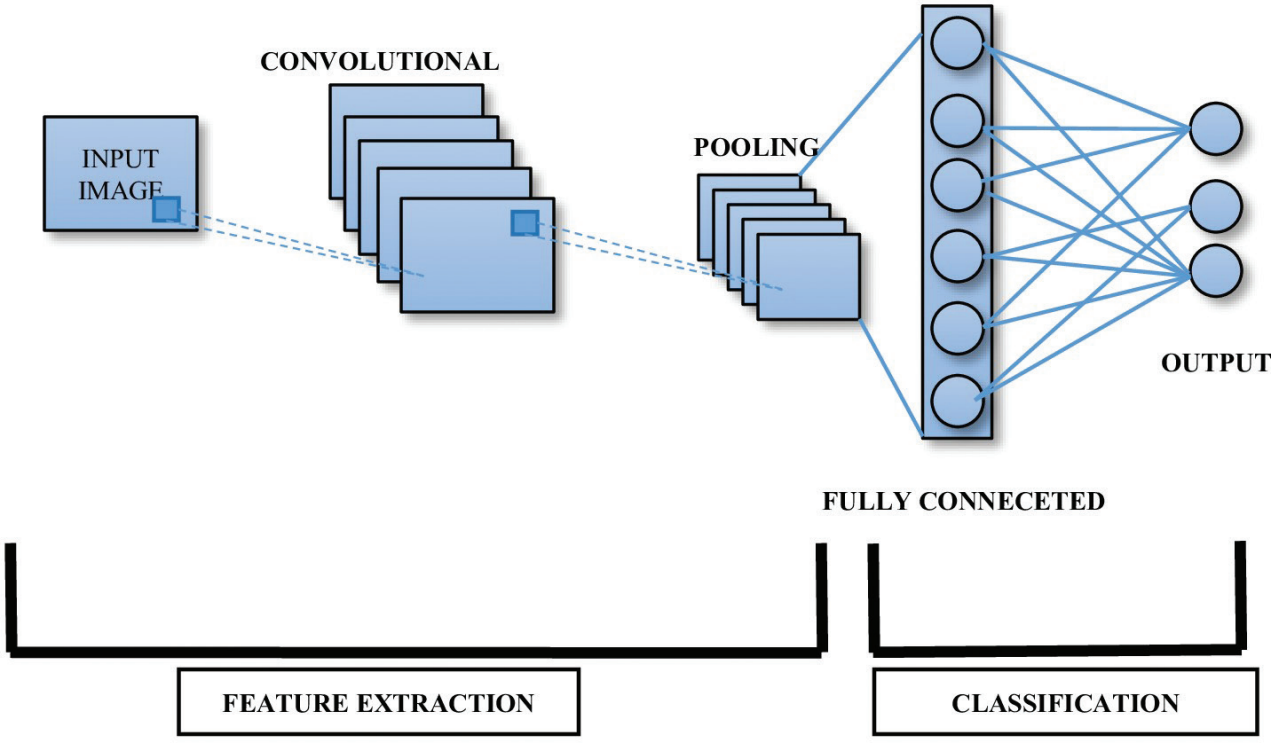

Figure 11: CNN architecture. CNN, convolutional neural network.

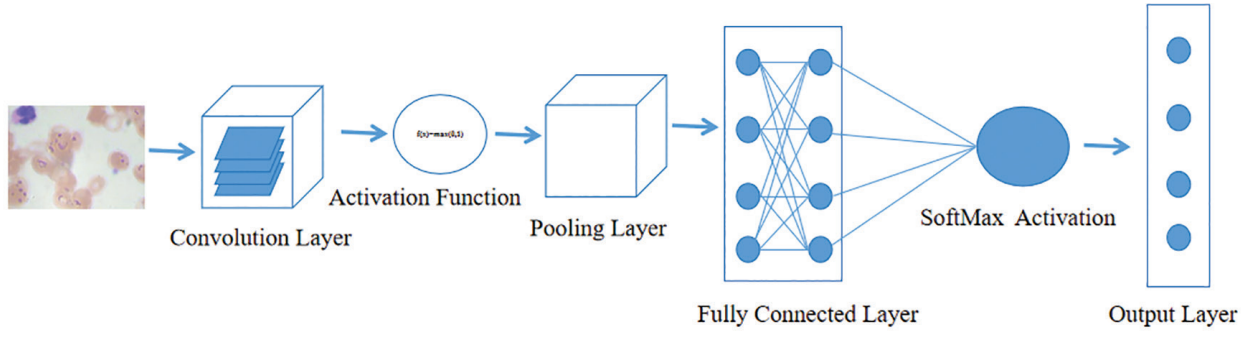

Figure 12: VGG16 architecture.

antibodies [34]. These white blood cells, including lymphocytes, are essential for antibody production and for combating bacterial and fungal infections. Additionally, research indicates that white blood cells have a relatively long lifespan [35, 36].

RBCs are the predominant type of blood cell [37]. On peripheral blood smears, they have a biconcave disc shape and contain cytoplasm abundant in hemoglobin, the crucial protein responsible for oxygen transport [17]. RBC have a critical role in transporting CO_2 from the peripheral tissues to the lungs for exhalation and O_2 from the lungs to the tissues [38]. Their unique structure enables efficient gas exchange between the tissues and lungs. The average lifespan of RBC is 120 days [33]. On the other hand, platelets (thrombocytes) are small, granular, nucleated cell fragments that are generated by megakaryocytes in the bone marrow [37] and are vital for hemostasis, working alongside plasma clotting factors [38, 39] Platelets have a

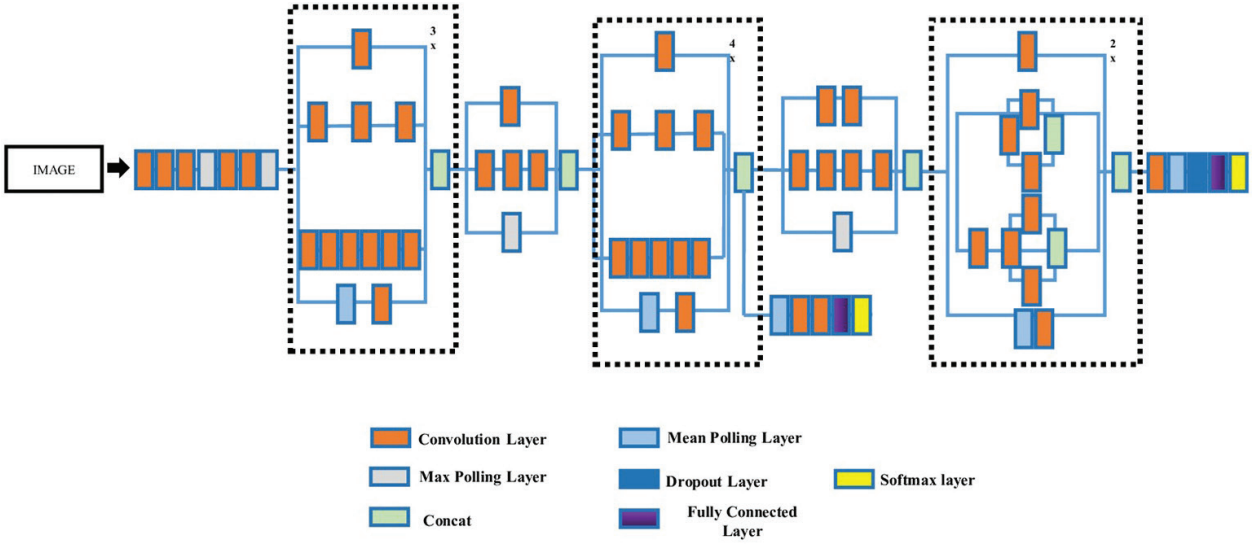

Figure 13: Inception V3 architecture.

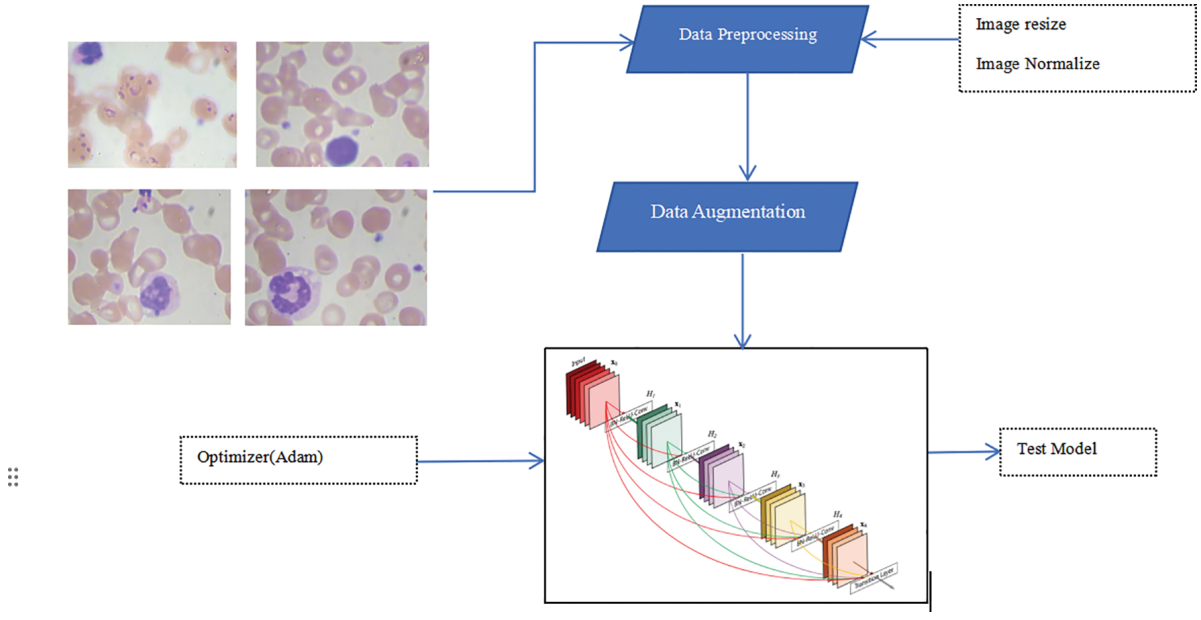

Figure 14: Applied framework.

shorter lifespan, ranging from 7 days to 10 days [40]. White blood cells, which come in various types [34]. include granulocytes derived from the bone marrow, which appear similar on a peripheral smear[40, 41]. Neutrophils, the most prevalent type of white blood cell, are easily recognizable by their light purple granules and a nucleus with three to five lobes. These phagocytes play a critical role in defending against acute infections [42].

h. Input image for model training

High-resolution images of blood cells were utilized as input images for machine-learning models in this study. Pre-processing of these images results in a 320 × 240-pixel standard, which is used to guarantee uniformity throughout the collection. One of four blood cell types—neutrophils, monocytes, lymphocytes, and eosinophils—is depicted in each illustration. With the datasets closer to balanced instances of

Table 2: About blood cells

Cell category	Size	Blood life span	Quantity of cells	Functions
RBC	6–8	120 days	Male:—4.5–6.5 × 10^6 Female 3.9–5.6 × 10^6	Conveyance of O_2 and CO_2
Thrombocytes	0.5–3.0	10 days	140-1,400 × 10^3	Coagulation
Phagocytes				
Neutrophils	12–15	6–10 hr	1.9–7.6 × 10^3 (48%–76%)	Protection against microorganisms such as fungi and bacteria
Monocytes	12–20	20–40 hr	0.2–0.8 × 10^3 (2.5%–8.5%)	Defense against pathogens like fungi and bacteria
Acidophils	12–15	Days	0.04–0.44 × 01^3 (<5%)	Defence from pathogens
Lymphocyte	7–9 (resting) 12–20 (active)	Weeks or years	1.5–3.5 × 10^3 (18%–41%)	B-cells: Assist in antibody production and the activation of T-cells. T-cells: Involved in viral defense and immune response

RBC, red blood cells.

different types of blood cells, the models can identify and extract features to identify and classify the blood cells during testing. Identification of blood cells is crucial for the early identification of anaemia and its types.

Monocytes are unequivocally the largest type of white blood cell, with diameters ranging from 12 μm to 20 μm [42]. They have a kidney-shaped or folded nucleus and bright blue cytoplasm with a few very small granules [43]. While monocytes are highly phagocytic like neutrophils, they differ significantly [44]. As they enter tissues, they transform into long-lived macrophages that are able to sense "danger" signals triggered by tissue damage or infections [45]. Eosinophils, named after the dawn goddess Eos, are distinguished by their numerous bright red cytoplasmic granules and two-lobed nuclei, with a diameter ranging from 12 μm to 15 μm [46]. They are crucial in chronic immune responses related to asthma, parasitic infections, and certain allergic reactions [47].

An essential component of the adaptive immune system is the lymphocyte [48]. They have a compact, spherical nucleus with little cytoplasm when they are dormant [49]. Their diameter ranges from 7 μm to 9 μm, similar to that of a typical RBC. However, when active, lymphocytes can expand up to 20 μm in size, featuring a larger nucleus, more cytoplasm, and a few granules [49]. Determining if circulating lymphocytes are natural killer cells, T cells, or B cells requires testing for specific lineage markers, as these types of lymphocytes cannot be distinguished with certainty based solely on their appearance [50]. The immune system's ability to "remember" previous pathogen exposures is supported by its durability and foundational structure.

IV. Result and Discussion

There are 3 Deep learning model has been used VGG16, InceptionV3, and DenseNet. By applying deep learning models, a significant level of results has been achieved. Table 3 presents a comparative analysis of the accuracy achieved by each deep learning model across different training epochs.

The evaluation matrix compares the performance of three deep learning models—VGG16, Inception V3, and DenseNet121—on a cell classification task involving EOSINOPHIL, LYMPHOCYTE, MONOCYTE, and NEUTROPHIL. It evaluates precision, recall, F1 score, and support. Precision represents the ratio of true positives to predicted positives, recall represents the ratio of true positives to actual positives, and the F1 score balances these metrics. DenseNet121 outperforms the others, with F1 scores between 0.85 and 0.98, while VGG16 scores range from 0.72 to 0.9, and Inception V3 from 0.67 to 0.9. Each class has around 500 samples. DenseNet121 demonstrates the best overall performance as shown in Figure 15.

a. Outcome InceptionV3 model

The InceptionV3 model was trained over 90 epochs with a batch size of 32. The training process yielded a

Table 3: Compare accuracy and time for each epoch based on three deep learning models

Model	Model parameters and results			
	Number of epochs	Accuracy (%)	Batch size	Time for each epoch (in ms)
VGG16	90	93.43	32	78 ms/step
DenseNet	90	90.48	32	89 ms/step
InceptionV3	90	78.80	32	100 ms/step

Evaluation Matrix															
Model	*VGG16*					*InceptionV3*					*DenseNet121*				
Class	*Precision*	*Recall*	*F1 Score*	*Support*	*Accuracy*	*Precision*	*Recall*	*F1 Score*	*Support*	*Accuracy*	*Precision*	*Recall*	*F1 Score*	*Support*	*Accuracy*
EOSINOPHIL	*0.91*	*0.89*	*0.90*	*501*	*0.88*	*0.73*	*0.67*	*0.70*	*501*	*0.67*	*0.85*	*0.86*	*0.85*	*501*	*0.88*
LYMPHOCYTE	*0.95*	*1*	*0.97*	*497*	*0.98*	*0.84*	*0.85*	*0.85*	*497*	*0.90*	*0.94*	*0.96*	*0.95*	*497*	*0.96*
MONOCYTE	*0.97*	*0.99*	*0.98*	*497*	*0.96*	*0.85*	*0.90*	*0.87*	*497*	*0.90*	*0.94*	*0.98*	*0.96*	*497*	*0.97*
NETUROPHIL	*0.91*	*0.86*	*0.89*	*500*	*0.86*	*0.73*	*0.73*	*0.73*	*500*	*0.73*	*0.89*	*0.82*	*0.85*	*500*	*0.93*

Figure 15: Evaluation metrics for deep learning models.

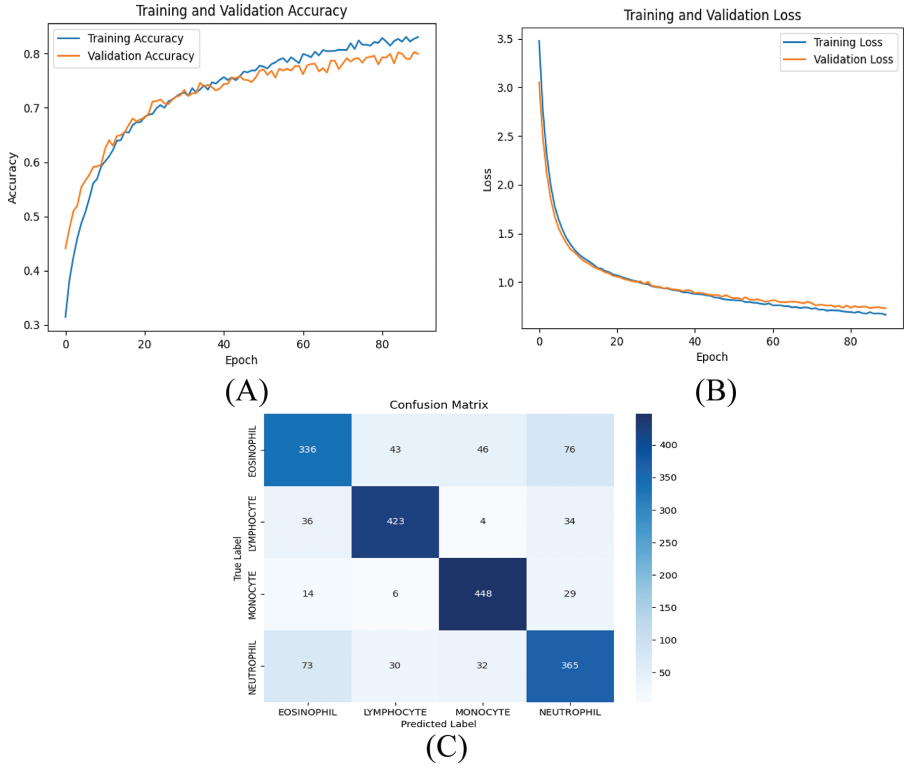

Figure 16: (A) presents the training and validation accuracy for each epoch, (B) shows the training and validation loss for each epoch, and (C) provides the confusion matrix for each class in the InceptionV3 Model.

final training accuracy of 83.04% and a test accuracy of 78.80%. The weighted average F1-score across all classes was 0.79, indicating good overall performance of the model as shown in Figure 16.

b. Outcomes VGG16 model

We developed a CNN model using the VGG16 architecture to classify four types of blood cells: neutrophils, monocytes, lymphocytes, and eosinophils. Training on a dataset of 9,957 images yielded an accuracy of 94.17% on the training set. For evaluation, a separate test set of 1995 images resulted in a loss of 0.4362 and an accuracy of 93.43%. Recall, F1- score, and precision calculations for every class indicated excellent performance as shown in Figure 17.

c. Outcomes DenseNet121

The DenseNet121 model was trained on a dataset of images containing the four classes of blood cells: Eosinophil, Lymphocyte, Monocyte, and Neutrophil. The model achieved a training accuracy of 91.32% and a test accuracy of 90.48% after 90 epochs as shown in Figure 18.

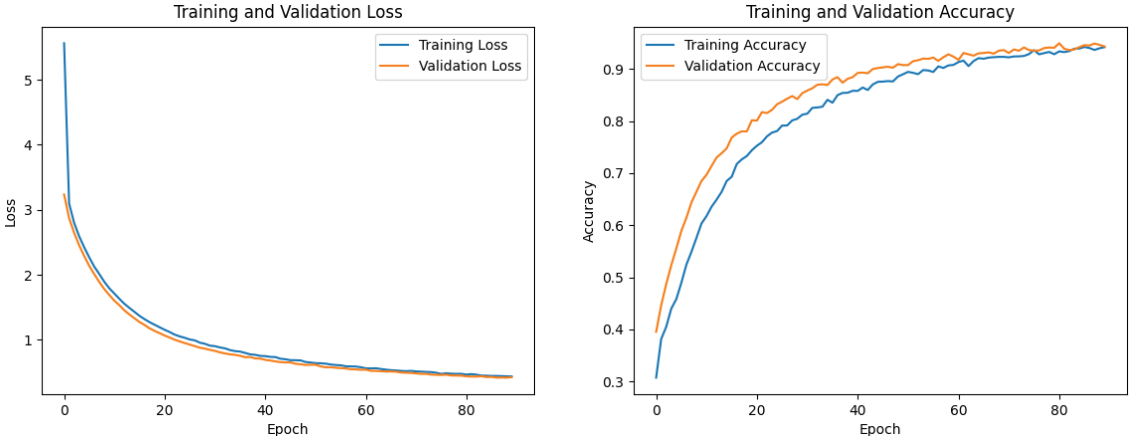

(A) (B)

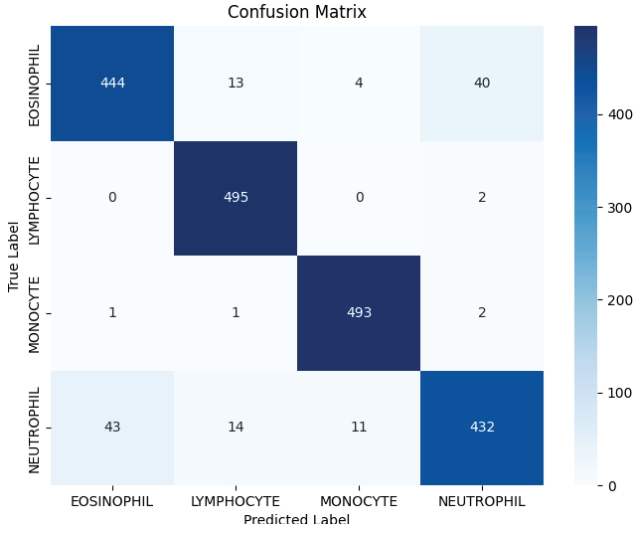

(C)

Figure 17: (A) presents the accuracy of training and validation for each epoch, (B) illustrates the loss during training and validation for each epoch, and (C) shows the confusion matrix for each class from the VGG16 Model.

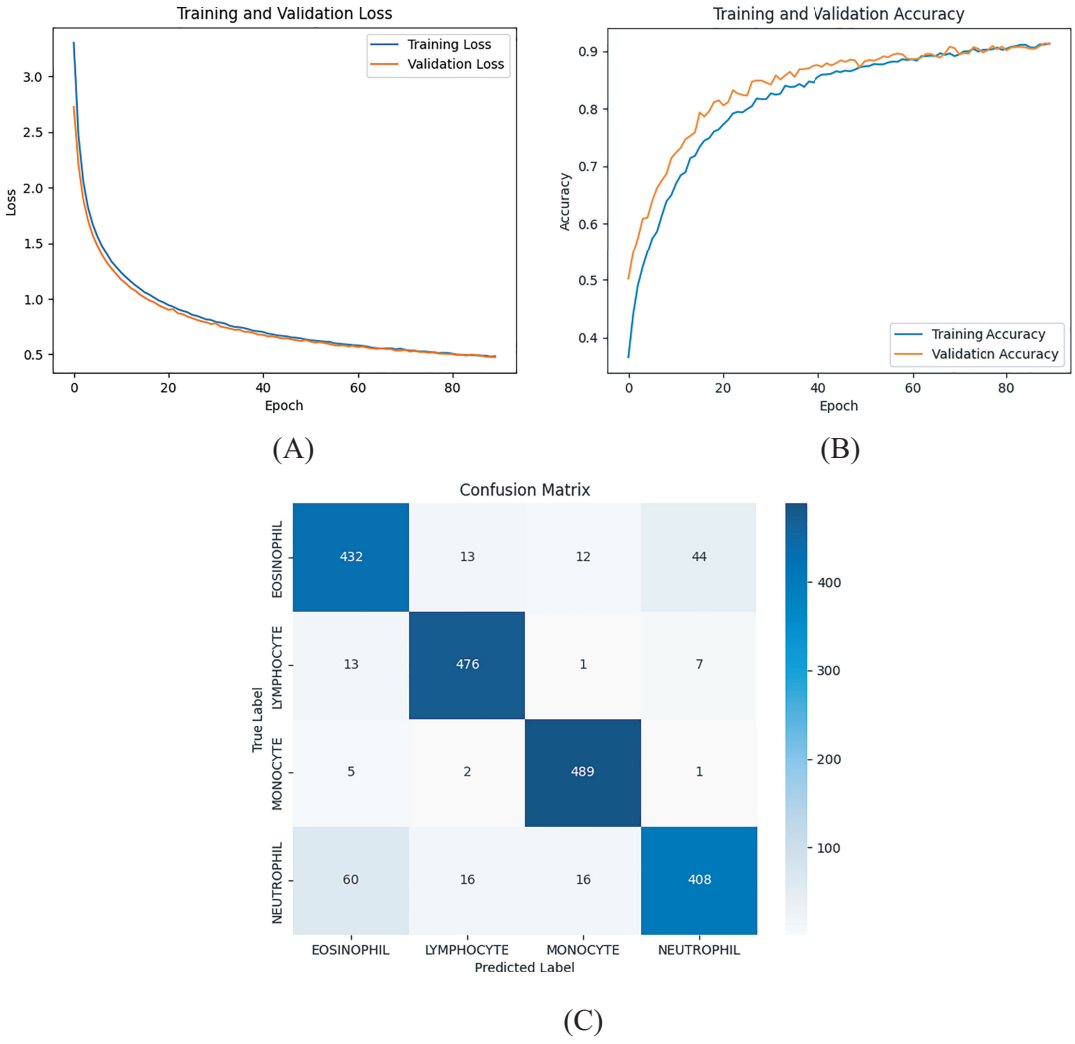

Figure 18: (A) presents the training and validation accuracy per epoch, (B) shows the training and validation loss for each epoch, and (C) provides the confusion matrix for each class from the DenseNET121 model.

V. Conclusion

In conclusion, our work illustrates how machine-learning models can be effectively employed to categorize different types of blood cells and leverage this information for the early detection of anaemia. Promising results were obtained when anaemia was accurately identified using blood cell pictures by the VGG16, InceptionV3, and DenseNet121 models. Particularly in susceptible populations like children and pregnant women, early identification of anaemia is essential for prompt intervention and treatment. Public health outcomes pertaining to anaemia could be greatly impacted by additional studies and the development of deep learning algorithms in this field.

VI. Future Work

The current study has demonstrated the effectiveness of deep learning models in categorizing blood cells and detecting anemia. We plan to enhance the dataset by incorporating more diverse samples from various geographical regions and broader demographics to improve the model's generalizability. This will also involve collecting images of additional blood cell types and other related hematological conditions. Extensive clinical trials and validations with larger, more varied patient populations will be essential to validate the model's effectiveness and reliability in real-world scenarios. Collaborating with medical professionals

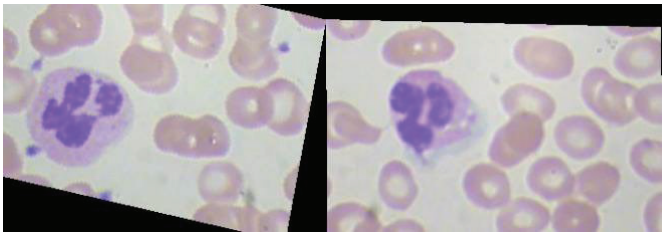

(A) Neutrophil

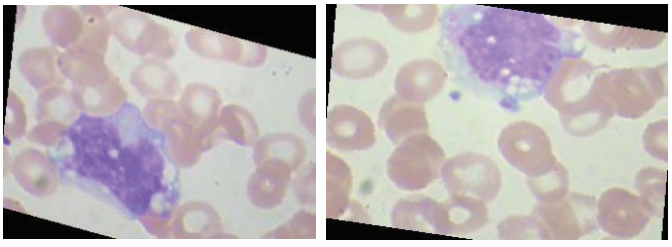

(B) Monocyte

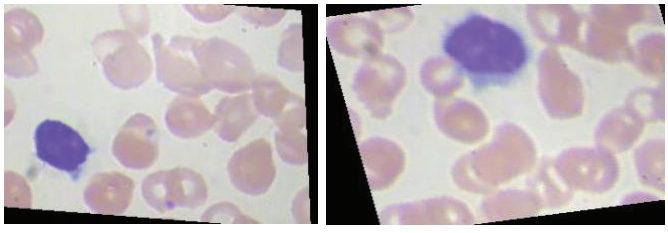

(C) Lymphocyte

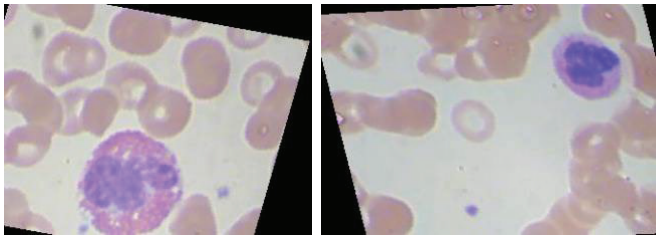

(D) Eosinophil

will ensure that the model meets clinical standards and requirements. Additionally, we aim to develop a real-time application for clinical use, integrating it with laboratory equipment and mobile devices for instant analysis and diagnosis. By addressing these areas, we aim to develop a robust, precise, and practical tool for detecting anemia and classifying blood cells, ultimately resulting in better patient outcomes and enhanced healthcare delivery.

Acknowledgment

The authors sincerely acknowledge the support provided by the Science for Equity Empowerment and Development scheme (SEED) under the Department of Science and Technology under grant: DST/SEED/CCRRC/2021/003/G.

Funding

We extend our heartfelt gratitude to symbiosis Institute of Technology Pune India for their generous financial assistance through the Symbiosis Research Support Fund (SRF) particularly articulated for this research paper. Their Support has been Instrumental in the successful completion of this research paper.

References

[1] J. W. Asare, P. Appiahene, and E. T. Donkoh, "Detection of anaemia using medical images: A comparative study of machine learning algorithms – A systematic literature review," *Inform Med Unlocked*, vol. 40, p. 101283, 2023, doi: 10.1016/j.imu.2023.101283.

[2] A. Bhatiasevi, "Anaemia Action Alliance," *World Health Organization*, 2015.

[3] S. Let, S. Tiwari, A. Singh, and M. Chakrabarty, "Prevalence and determinants of anaemia among women of reproductive age in Aspirational Districts of India: an analysis of NFHS 4 and NFHS 5 data," *BMC Public Health*, vol. 24, no. 1, p. 437, Feb. 2024, doi: 10.1186/s12889-024-17789-3.

[4] B. S. Maner and L. Moosavi, *Mean Corpuscular Volume*. 2024.

[5] S. Gul and M. S. Khan, "A Survey of Audio Enhancement Algorithms for Music, Speech, Bioacoustics, Biomedical, Industrial, and Environmental Sounds by Image U-Net," *IEEE Access*, vol. 11, pp. 144456–144483, 2023, doi: 10.1109/ACCESS.2023.3344813.

[6] A. Gupta *et al.*, "Risk factors of anemia amongst elderly population living at high-altitude region of India," *J Family Med Prim Care*, vol. 9, no. 2, p. 673, 2020, doi: 10.4103/jfmpc.jfmpc_468_19.

[7] S. K. Singh, H. Lhungdim, C. Shekhar, L. K. Dwivedi, S. Pedgaonkar, and K. S. James, "Key drivers of reversal of trend in childhood anaemia in India: evidence from Indian demographic and health surveys, 2016–21," *BMC Public Health*, vol. 23, no. 1, p. 1574, Aug. 2023, doi: 10.1186/s12889-023-16398-w.

[8] P. Appiahene *et al.*, "Application of ensemble models approach in anemia detection using images of the palpable palm," *Med Nov Technol Devices*, vol. 20, p. 100269, Dec. 2023, doi: 10.1016/j.medntd.2023.100269.

[9] M. Zuin, G. Rigatelli, L. Quadretti, L. Fogato, G. Zuliani, and L. Roncon, "Prognostic Role of Anemia in COVID-19 Patients: A Meta-Analysis," *Infect Dis Rep*, vol. 13, no. 4, pp. 930–937, Oct. 2021, doi: 10.3390/idr13040085.

[10] R. Bellmann-Weiler *et al.*, "Prevalence and Predictive Value of Anemia and Dysregulated Iron Homeostasis in Patients with COVID-19 Infection," *J Clin Med*, vol. 9, no. 8, p. 2429, Jul. 2020, doi: 10.3390/jcm9082429.

[11] S. Dhalla *et al.*, "Semantic segmentation of palpebral conjunctiva using predefined deep neural architectures for anemia detection," *Procedia Comput Sci*, vol. 218, pp. 328–337, 2023, doi: 10.1016/j.procs.2023.01.015.

[12] P. T. Dalvi and N. Vernekar, "Anemia detection using ensemble learning techniques and statistical models," in *2016 IEEE International Conference on Recent Trends in Electronics, Information & Communication Technology (RTEICT)*, IEEE, May 2016, pp. 1747–1751. doi: 10.1109/RTEICT.2016.7808133.

[13] J. W. Asare, P. Appiahene, E. T. Donkoh, and G. Dimauro, "Iron deficiency anemia detection using machine learning models: A comparative study of fingernails, palm and conjunctiva of the eye images," *Engineering Reports*, vol. 5, no. 11, Nov. 2023, doi: 10.1002/eng2.12667.

[14] J. W. Asare, W. L. Brown-Acquaye, M. M. Ujakpa, E. Freeman, and P. Appiahene, "Application of machine learning approach for iron deficiency anaemia detection in children using conjunctiva images," *Inform Med Unlocked*, vol. 45, p. 101451, 2024, doi: 10.1016/j.imu.2024.101451.

[15] P. Appiahene, J. W. Asare, E. T. Donkoh, G. Dimauro, and R. Maglietta, "Detection of iron deficiency anemia by medical images: a comparative study of machine learning algorithms," *BioData Min*, vol. 16, no. 1, p. 2, Jan. 2023, doi: 10.1186/s13040-023-00319-z.

[16] A. Kesarwani, S. Das, D. R. Kisku, and M. Dalui, "Dual mode information fusion with pre-trained CNN models and transformer for video-based non-invasive anaemia detection," *Biomed Signal Process*

Control, vol. 88, p. 105592, Feb. 2024, doi: 10.1016/j.bspc.2023.105592.

[17] El-Sayed M. Towfek El-kenawy, "A Machine Learning Model for Hemoglobin Estimation and Anemia Classification," in *International Journal of Computer Science and Information Security*, International Journal of Computer Science and Information Security, Feb. 2019, pp. 100–108.

[18] J. R. Khan, S. Chowdhury, H. Islam, and E. Raheem, "Machine Learning Algorithms To Predict The Childhood Anemia In Bangladesh," *Journal of Data Science*, vol. 17, no. 1, pp. 195–218, Feb. 2021, doi: 10.6339/JDS.201901_17(1)0.0009.

[19] M. Jaiswal, A. Srivastava, and T. J. Siddiqui, "Machine Learning Algorithms for Anemia Disease Prediction," 2019, pp. 463–469. doi: 10.1007/978-981-13-2685-1_44.

[20] S. KILICARSLAN, M. CELIK, and Ş. SAHIN, "Hybrid models based on genetic algorithm and deep learning algorithms for nutritional Anemia disease classification," *Biomed Signal Process Control*, vol. 63, p. 102231, Jan. 2021, doi: 10.1016/j.bspc.2020.102231.

[21] Y. Chen, K. Zhong, Y. Zhu, and Q. Sun, "Two-stage hemoglobin prediction based on prior causality," *Front Public Health*, vol. 10, Nov. 2022, doi: 10.3389/fpubh.2022.1079389.

[22] S. M. Sarsam, H. Al-Samarraie, A. I. Alzahrani, and A. S. Shibghatullah, "A non-invasive machine learning mechanism for early disease recognition on Twitter: The case of anemia," *Artif Intell Med*, vol. 134, p. 102428, Dec. 2022, doi: 10.1016/j.artmed.2022.102428.

[23] S. Yeruva, M. S. Varalakshmi, B. P. Gowtham, Y. H. Chandana, and PESN. K. Prasad, "Identification of Sickle Cell Anemia Using Deep Neural Networks," *Emerging Science Journal*, vol. 5, no. 2, pp. 200–210, Apr. 2021, doi: 10.28991/esj-2021-01270.

[24] A. Tamir *et al.*, "Detection of anemia from image of the anterior conjunctiva of the eye by image processing and thresholding," in *2017 IEEE Region 10 Humanitarian Technology Conference (R10-HTC)*, IEEE, Dec. 2017, pp. 697–701. doi: 10.1109/R10-HTC.2017.8289053.

[25] M. Wang *et al.*, "Toward an optimal kernel extreme learning machine using a chaotic moth-flame optimization strategy with applications in medical diagnoses," *Neurocomputing*, vol. 267, pp. 69–84, Dec. 2017, doi: 10.1016/j.neucom.2017.04.060.

[26] M. Wang and H. Chen, "Chaotic multi-swarm whale optimizer boosted support vector machine for medical diagnosis," *Appl Soft Comput*, vol. 88, p. 105946, Mar. 2020, doi: 10.1016/j.asoc.2019.105946.

[27] M. Yang, P. Kumar, J. Bhola, and M. Shabaz, "Development of image recognition software based on artificial intelligence algorithm for the efficient sorting of apple fruit," *International Journal of System Assurance Engineering and Management*, vol. 13, no. S1, pp. 322–330, Mar. 2022, doi: 10.1007/s13198-021-01415-1.

[28] C. Szegedy, V. Vanhoucke, S. Ioffe, J. Shlens, and Z. Wojna, "Rethinking the Inception Architecture for Computer Vision," in *2016 IEEE Conference on Computer Vision and Pattern Recognition (CVPR)*, IEEE, Jun. 2016, pp. 2818–2826. doi: 10.1109/CVPR.2016.308.

[29] D. T. B. I. D. and J. D. V. Provan, *Oxford Handbook of Clinical Haematology*, 4th ed. Uk: Oxford University press, 2015.

[30] J.-B. Michel and J. L. Martin-Ventura, "Red Blood Cells and Hemoglobin in Human Atherosclerosis and Related Arterial Diseases," *Int J Mol Sci*, vol. 21, no. 18, p. 6756, Sep. 2020, doi: 10.3390/ijms21186756.

[31] B. Savkovic *et al.*, "Comparative Characteristics of Ductile Iron and Austempered Ductile Iron Modeled by Neural Network," *Materials*, vol. 12, no. 18, p. 2864, Sep. 2019, doi: 10.3390/ma12182864.

[32] M. Duan, K. Li, X. Liao, and K. Li, "A Parallel Multiclassification Algorithm for Big Data Using an Extreme Learning Machine," *IEEE Trans Neural Netw Learn Syst*, vol. 29, no. 6, pp. 2337–2351, Jun. 2018, doi: 10.1109/TNNLS.2017.2654357.

[33] T. Yoshida, M. Prudent, and A. D'alessandro, "Red blood cell storage lesion: causes and potential clinical consequences.," *Blood Transfus*, vol. 17, no. 1, pp. 27–52, Jan. 2019, doi: 10.2450/2019.0217-18.

[34] A. R. Andrade, L. H. S. Vogado, R. de M. S. Veras, R. R. V. Silva, F. H. D. Araujo, and F. N. S. Medeiros, "Recent computational methods for white blood cell nuclei segmentation: A comparative study," *Comput Methods Programs Biomed*, vol. 173, pp. 1–14, May 2019, doi: 10.1016/j.cmpb.2019.03.001.

[35] J. C. Chavez, C. Bachmeier, and M. A. Kharfan-Dabaja, "CAR T-cell therapy for B-cell lymphomas: clinical trial results of available products," *Ther Adv Hematol*, vol. 10, p. 204062071984158, Jan. 2019, doi: 10.1177/2040620719841581.

[36] L. Jiang, C. Tang, and H. Zhou, "White blood cell classification via a discriminative region detection assisted feature aggregation network," *Biomed Opt Express*, vol. 13, no. 10, p. 5246, Oct. 2022, doi: 10.1364/BOE.462905.

[37] X. Han, C. Wang, and Z. Liu, "Red Blood Cells as Smart Delivery Systems," *Bioconjug Chem*, vol. 29, no. 4, pp. 852–860, Apr. 2018, doi: 10.1021/acs.bioconjchem.7b00758.

[38] Q. Xia, Y. Zhang, Z. Li, X. Hou, and N. Feng, "Red blood cell membrane-camouflaged nanoparticles: a novel drug delivery system for antitumor application," *Acta Pharm Sin B*, vol. 9, no. 4, pp. 675–689, Jul. 2019, doi: 10.1016/j.apsb.2019.01.011.

[39] L. Guo and M. T. Rondina, "The Era of Thromboinflammation: Platelets Are Dynamic Sensors and Effector Cells During Infectious Diseases,"

Front Immunol, vol. 10, Sep. 2019, doi: 10.3389/fimmu.2019.02204.

[40] A. W. Anz, R. Hubbard, N. K. Rendos, P. A. Everts, J. R. Andrews, and J. G. Hackel, "Bone Marrow Aspirate Concentrate Is Equivalent to Platelet-Rich Plasma for the Treatment of Knee Osteoarthritis at 1 Year: A Prospective, Randomized Trial," *Orthop J Sports Med*, vol. 8, no. 2, p. 232596711990095, Feb. 2020, doi: 10.1177/2325967119900958.

[41] C. Crotti, E. Agape, A. Becciolini, M. Biggioggero, and E. G. Favalli, "Targeting Granulocyte-Monocyte Colony-Stimulating Factor Signaling in Rheumatoid Arthritis: Future Prospects," *Drugs*, vol. 79, no. 16, pp. 1741–1755, Nov. 2019, doi: 10.1007/s40265-019-01192-z.

[42] C. Silvestre-Roig, Z. G. Fridlender, M. Glogauer, and P. Scapini, "Neutrophil Diversity in Health and Disease," *Trends Immunol*, vol. 40, no. 7, pp. 565–583, Jul. 2019, doi: 10.1016/j.it.2019.04.012.

[43] P. B. Narasimhan, P. Marcovecchio, A. A. J. Hamers, and C. C. Hedrick, "Nonclassical Monocytes in Health and Disease," *Annu Rev Immunol*, vol. 37, no. 1, pp. 439–456, Apr. 2019, doi: 10.1146/annurev-immunol-042617-053119.

[44] B. V. Rooney, A. B. Bigley, E. C. LaVoy, M. Laughlin, C. Pedlar, and R. J. Simpson, "Lymphocytes and monocytes egress peripheral blood within minutes after cessation of steady state exercise: A detailed temporal analysis of leukocyte extravasation," *Physiol Behav*, vol. 194, pp. 260–267, Oct. 2018, doi: 10.1016/j.physbeh.2018.06.008.

[45] J. Florentin *et al.*, "Inflammatory Macrophage Expansion in Pulmonary Hypertension Depends upon Mobilization of Blood-Borne Monocytes," *The Journal of Immunology*, vol. 200, no. 10, pp. 3612–3625, May 2018, doi: 10.4049/jimmunol.1701287.

[46] A. D. Klion, S. J. Ackerman, and B. S. Bochner, "Contributions of Eosinophils to Human Health and Disease," *Annual Review of Pathology: Mechanisms of Disease*, vol. 15, no. 1, pp. 179–209, Jan. 2020, doi: 10.1146/annurev-pathmechdis-012419-032756.

[47] K. Nakagome and M. Nagata, "Involvement and Possible Role of Eosinophils in Asthma Exacerbation," *Front Immunol*, vol. 9, Sep. 2018, doi: 10.3389/fimmu.2018.02220.

[48] G. E. Idos, J. Kwok, N. Bonthala, L. Kysh, S. B. Gruber, and C. Qu, "The Prognostic Implications of Tumor Infiltrating Lymphocytes in Colorectal Cancer: A Systematic Review and Meta-Analysis," *Sci Rep*, vol. 10, no. 1, p. 3360, Feb. 2020, doi: 10.1038/s41598-020-60255-4.

[49] S. Gavrilov, K. Zhudenkov, G. Helmlinger, J. Dunyak, K. Peskov, and S. Aksenov, "Longitudinal Tumor Size and Neutrophil-to-Lymphocyte Ratio Are Prognostic Biomarkers for Overall Survival in Patients with Advanced Non-Small Cell Lung Cancer Treated with Durvalumab," *CPT Pharmacometrics Syst Pharmacol*, vol. 10, no. 1, pp. 67–74, Jan. 2021, doi: 10.1002/psp4.12578.

[50] A. D. Cohen *et al.*, "B cell maturation antigen–specific CAR T cells are clinically active in multiple myeloma," *Journal of Clinical Investigation*, vol. 129, no. 6, pp. 2210–2221, Apr. 2019, doi: 10.1172/JCI126397.